Effects of available long offset and random noise on simultaneous-AVO inversion

Sergio Romahn and Kris Innanen

ABSTRACT

The purpose of this work is to understand how the maximum offset available and the level of noise impact together the performance of simultaneous-AVO inversion, specifically when extracting S-impedance information. A low 30-m-thick gas sand reservoir, with a Class-III AVO anomaly, constitutes the geological framework. The evaluation is focused on the ability of separating the gas reservoir from the background (shale layers and brine sands) in a P- vs S-impedance plot. We took the original logs from the well as reference to measure the root mean square error (RMSE) of the inverted P- and S-impedance logs. The combined error in a P- vs S-impedance crossplot is represented by the multiplication of the inverted P- and S-impedance errors. Firstly, we analyzed the scenario with no noise while reducing the maximum offset or angle of incidence. The points that correspond to the reservoir, in the P- vs S- impedance plot, tend to be more disperse and closer to the background as the maximum offset available is reduced. The extraction of S-wave information is strongly affected under this scenario. The best reservoir discrimination in the P- vs S impedance crossplot is given when we use angles between 40 and 45 degrees. Although we cannot estimate accurate values of the P- vs S-impedance points when we use maximum angles lower than 40 degrees, we are still able to discriminate the gas reservoir from the background. The reservoir points tend to be close to the background when we use maximum angles lower than 30 degrees. In the second part of this experiment, we revised the scenario of varying the level of noise while keeping the maximum angle of 45 degrees constant. Signal to noise ratios (S/N) lower than 4 produce a considerable dispersion of the P- vs S- impedance points. Finally, we plotted the error as a function of noise and maximum angle in order to observe the combined effect of these two factors. Based on the reservoir discrimination, we classified the combined effect of maximum offset available and noise in four categories: best, acceptable, risky and non-acceptable results. The best results are produced with S/N greater than 7 and maximum angles between 40 and 45 degrees. Acceptable results arise for a S/N between 3 and 7 and maximum angles greater than 30 degrees; and with maximum angles between 30 and 40 with S/N greater than 7. Risky results are produced with S/N lower than 3 and angles smaller than 30 degrees. The results are non-acceptable if we have maximum angles of incidence smaller then 25 degrees. We also observed that angles greater than 45 degrees may deteriorate the inversion result.

INTRODUCTION

The aim of simultaneous-AVO inversion is to extract S-wave and density information from PP pre-stack seismic data. The availability of this information may be the key to discriminate reservoirs from the background in some geological frameworks, as the one shown in Fig. 1 that corresponds to the gas reservoir analyzed in this work. We can see that the acoustic solution for this problem would not be enough to identify the reservoir. The P-impedance range of the reservoir overlaps with the background's P-impedance.

However, if we consider P- and S-impedances together, we are able to appropriately separate the reservoir from the background. This fact constitutes a motivation for acquiring seismic data capable to provide S-wave information by applying seismic inversion techniques such as simultaneous-AVO inversion.

We applied the simultaneous inversion approach given by Hampson et-al (2005). They use an initial impedance model which is iteratively perturbed until density, P- impedance and S-impedance are found. The algorithm applies a reformulation given by Fatti (1994) of the Aki and Richards' approximation for the Zoeppritz equations (Aki and Richards, 2002). The authors assume that: 1) the linearized approximation for reflectivity holds, 2) PP reflectivity as a function of angle can be given by the Aki-Richards equations, and 3) there is a linear relationship between the logarithm of P-impedance and both S-impedance and density. The presence of random noise and the lack of large angles will challenge the first and second assumptions.

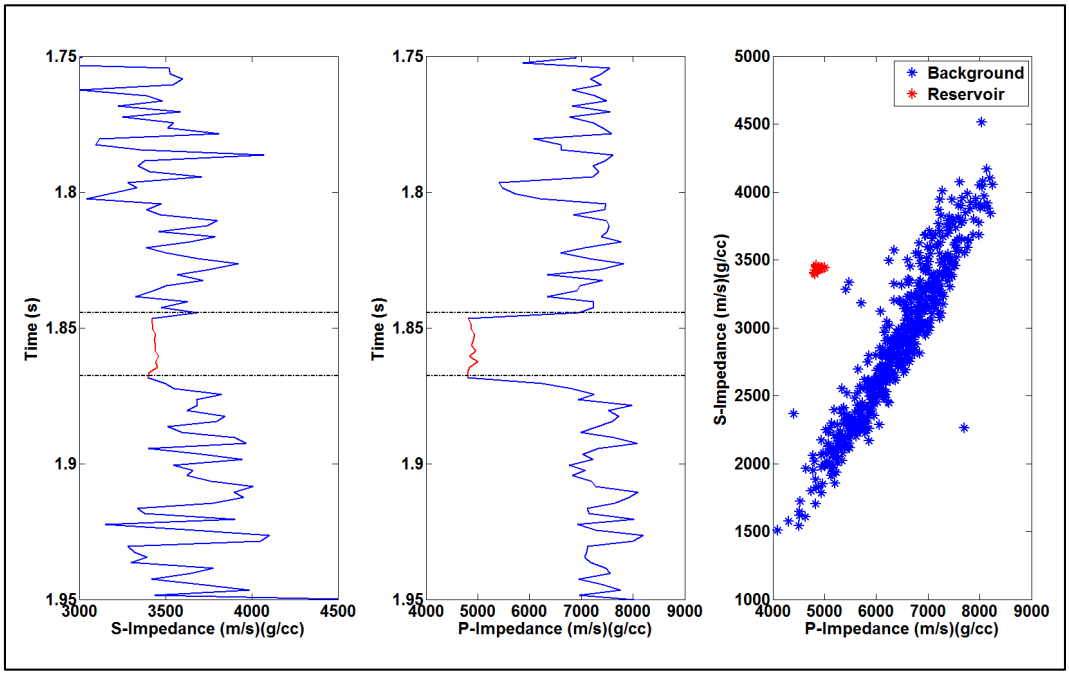

FIG. 1. Log data of a gas-producing well. Density, P- and S-wave velocity logs were used for this experiment.

The maximum offset (or angle of incidence) is a critical parameter in seismic data acquisition. Geophysicists typically design this parameter as a function of the deeper target or taking into account the processing mute (Cordsen et-al, 2000; Galbraith, 2004). The need for long offset information so that we can successfully apply AVO inversion may become another criterion when designing seismic surveys. The importance of this parameter for AVO inversion was pointed out by Stolt and Weglein (1985). They mentioned the requirement of a large range of offset angles for applying this technique, and they also warned about the fact that angles too large may break down the linearized model. On the other hand, the impact of random noise in AVO inversion has been analyzed by authors such as Downton and Lines (2001). They proposed a methodology to know the feasibility of applying AVO inversion in the presence of noise. We intend to

understand the concurrent impact of random noise and maximum offset available on AVO inversion.

Fig. 2 shows the geological target which is a 30-m sand reservoir producing gas at a depth of 2280 m. A Ricker wavelet with a dominant frequency of 25 Hz resolves the top and the base of the reservoir within the quarter-wavelength criterion.

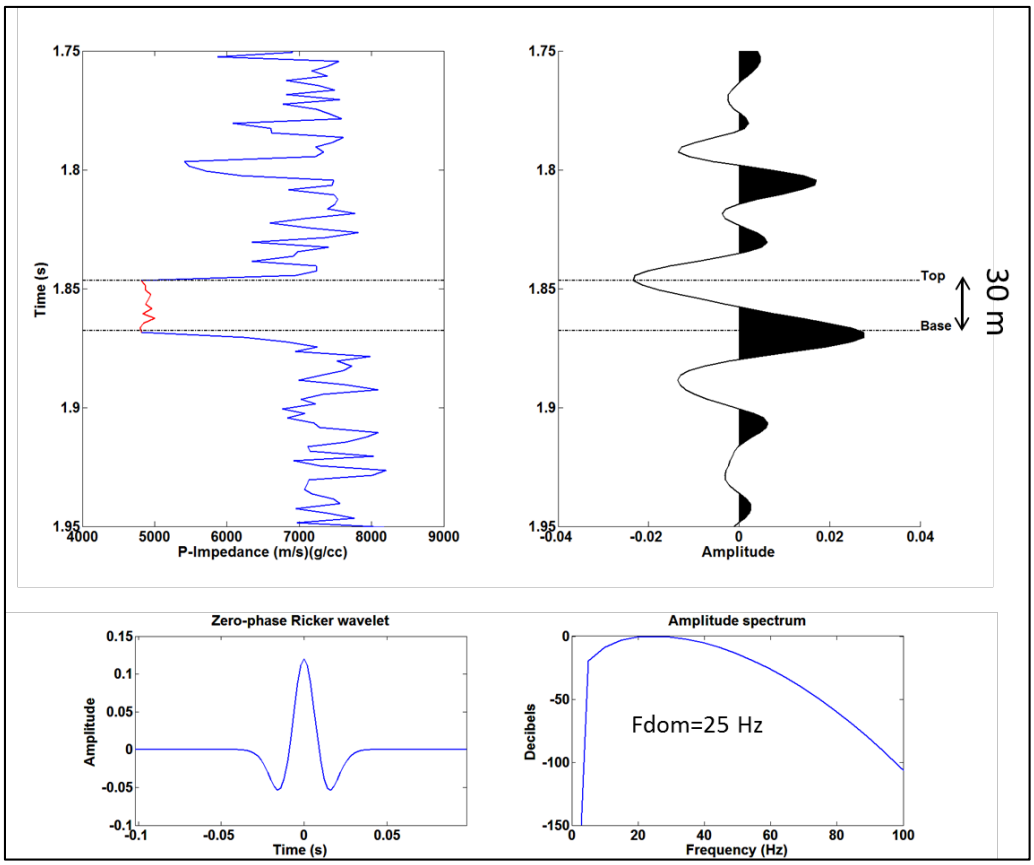

FIG. 2. The geological target is a 30-m sand reservoir that produces gas. A Ricker wavelet of 25 Hz of dominant frequency resolves the top and the base of the reservoir.

The top and base reflection coefficient variations with angle, given by the Zoeppritz equation, are shown in Fig. 3. We observe a subtle increment of the reflection coefficient amplitude between angles from 1 to 20 degrees. The reflection coefficients moderately rise from 20 to 40 degrees. The amplitude abruptly increases with angles greater than 45 degrees and up to the critical angle at 58 degrees. We know the relationship between offset and angle of incidence by using ray tracing. The offset that corresponds to the critical angles is 4100 m. We used pre-critical angles lower than 50 degrees (3670 m of offset) in this work.

Figure 4 shows the synthetic gather with AVO response constructed by using the density, P-wave and S-wave velocity logs, the Zoeppritz equations, and the zero-phase Ricker wavelet. The AVO response corresponds to a class III. We used this seismic angle gather to examine the effect of reducing the angle of incidence and the impact of varying the signal to noise ratio.

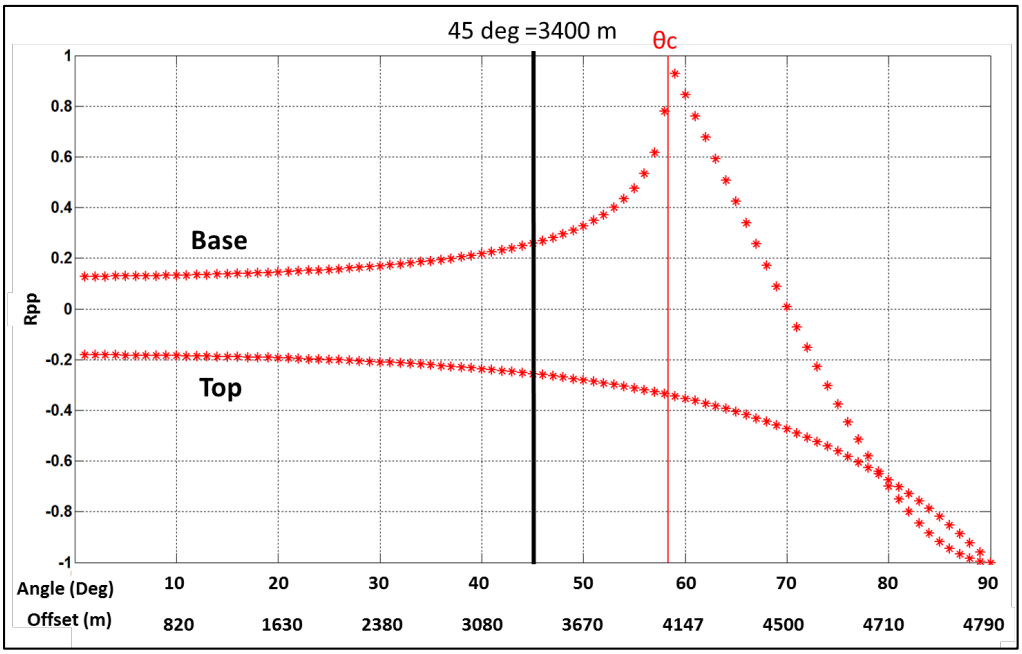

Fig. 3 Reflection coefficient variation with angle (and offset). The critical angle is 58 degrees. Pre-critical angles traces up to 50 degrees were used in this experiment.

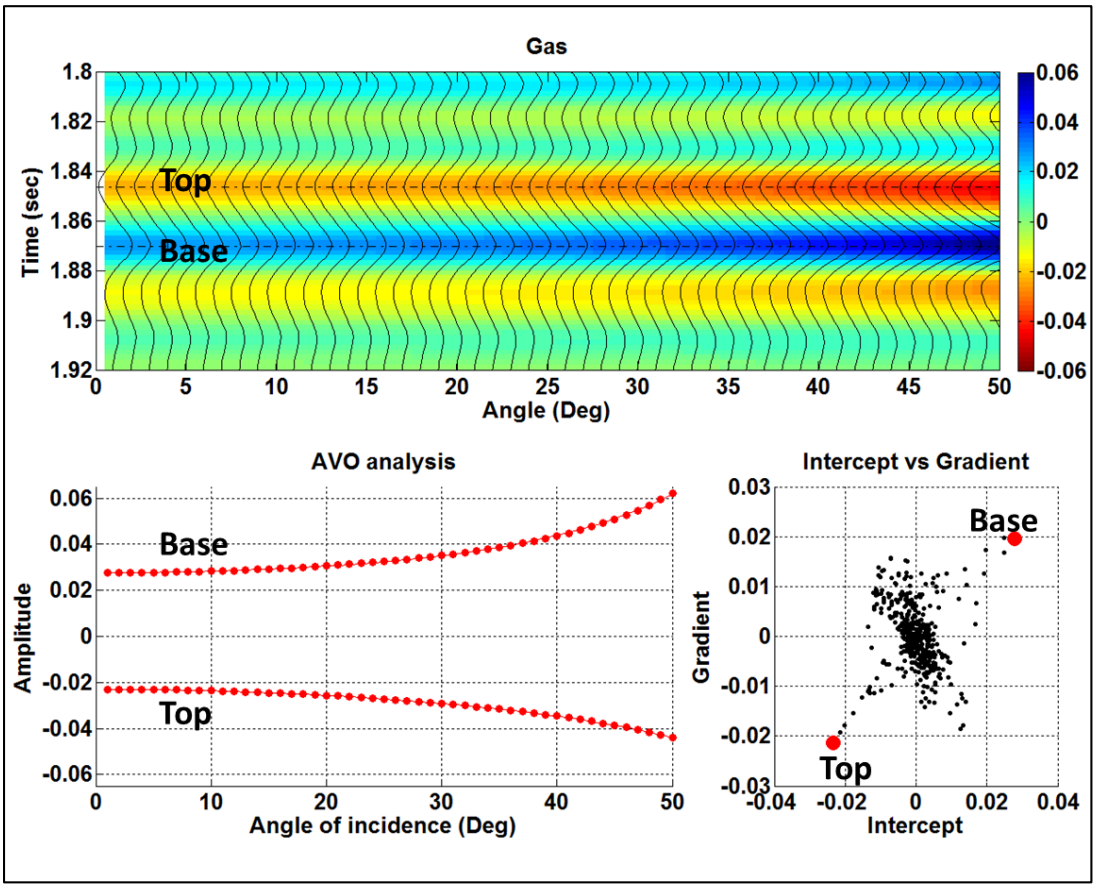

FIG. 4. Synthetic angle gather showing an amplitude increment given the presence of gas. The intercept vs gradient plot shows a typical class-III anomaly.

LABORATORY PROCEDURE AND DATA ANALYSIS

Simultaneous-AVO inversion

We used the synthetic seismic gather with no noise (showed in Fig. 4) to apply simultaneous-AVO inversion. Inverted P- and S- impedance logs were obtained from this process. All other factors that may influence the performance of the inversion process were kept constant. Examples of these factors are: Vp/Vs, the logarithm relationship between P-impedance with both density and S-impedance, and the tolerance within the conjugate gradient method. The RMSE was calculated in a window around the target between 1.83 and 1.89 seconds. The original logs were taken as reference for this purpose. Fig. 5 shows, in the first and second tracks, the original impedance logs in blue, the inverted logs in red, and the initial low frequency model in black. The original and inverted seismic traces (for 1, 15, 30 and 45 degrees) are also shown in tracks 4 and 5, respectively. The fifth track shows the difference between the original and inverted seismic traces. We used an angle range from 1 to 45 degrees for this case. A low-pass filter with a cut-off of 60 Hz was applied to the original logs to be compared to the inverted logs.

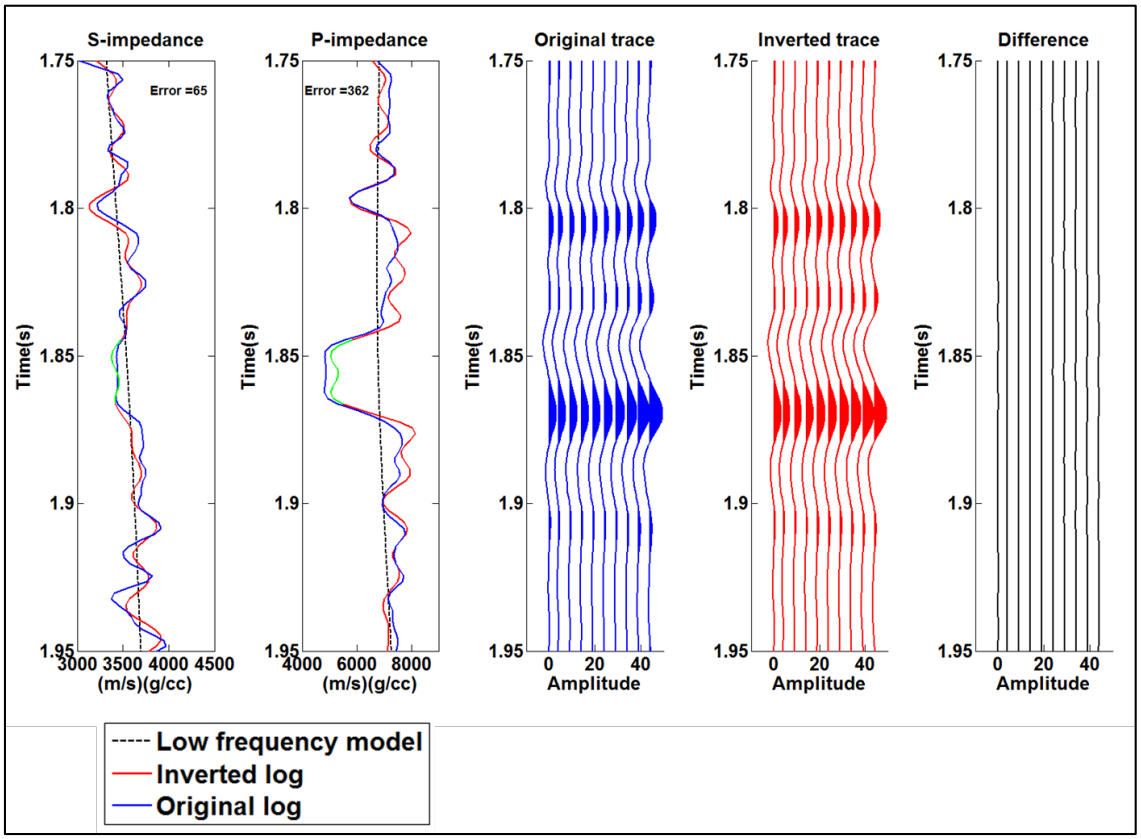

FIG. 5. Simultaneous-AVO inversion applied to the synthetic gather of Fig. 4. No noise was added. We used an angle range from 1 to 45 degrees.

The inverted and original P- and S-impedance logs were crossplotted together in Fig. 6. The reservoir points are highlighted in green. The error was calculated by multiplying

the RMSE of the inverted P- and S-impedances. In this case, we can discriminate the reservoir from the background in a similar way as the original logs do.

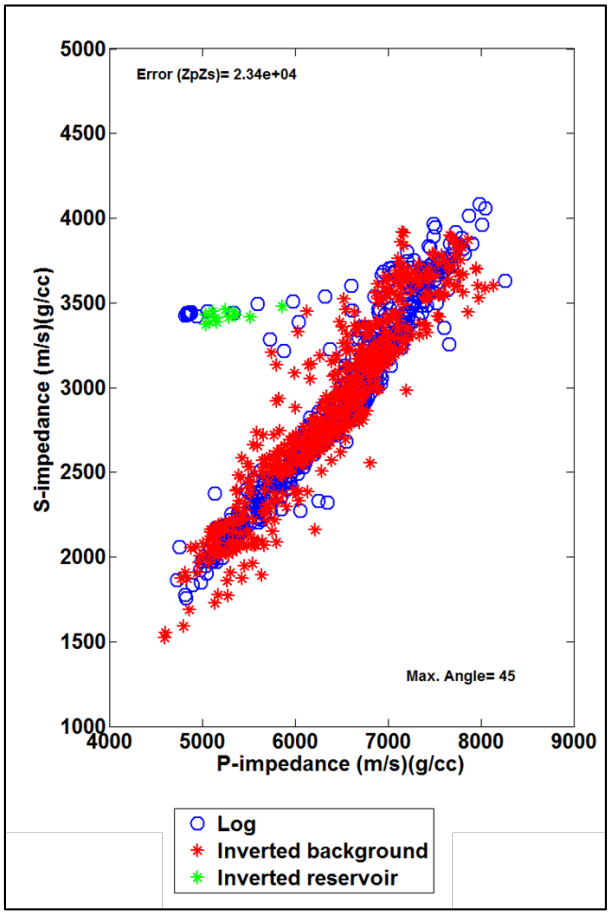

FIG. 6 Comparison between the inverted and original P- vs S- impedance plot. The reservoir is shown in green. We can discriminate the reservoir from the background. This case corresponds to maximum angles of 45 degrees, without noise.

Effect of reducing the maximum angle of incidence in simultaneous-AVO inversion

Fig. 7 shows the effect of reducing the maximum angle of incidence in the performance of simultaneous-AVO inversion. No noise was added in this case. We observe that the lack of large angles negatively affects the ability of extracting S-impedance information, especially when the maximum angle available is smaller than 35 degrees. The inverted P-impedance is moderately affected when we reduce the maximum available angle. Angle traces greater than 35 and up to 45 degrees favour the P-impedance estimation. The P- vs S-impedance plot shows how the reservoir is better discriminated if we use progressively larger angle traces. This is true for maximum angles up to 45 degrees. When we add angle traces greater than 45 degrees, the discrimination deteriorates and the error increases, as it is shown in Fig. 8.

Fig. 8 shows the normalized root mean square error for the inverted S- and P-impedances, and the combined error. The combined error denotes what happens in the P- vs S-impedance crossplot.

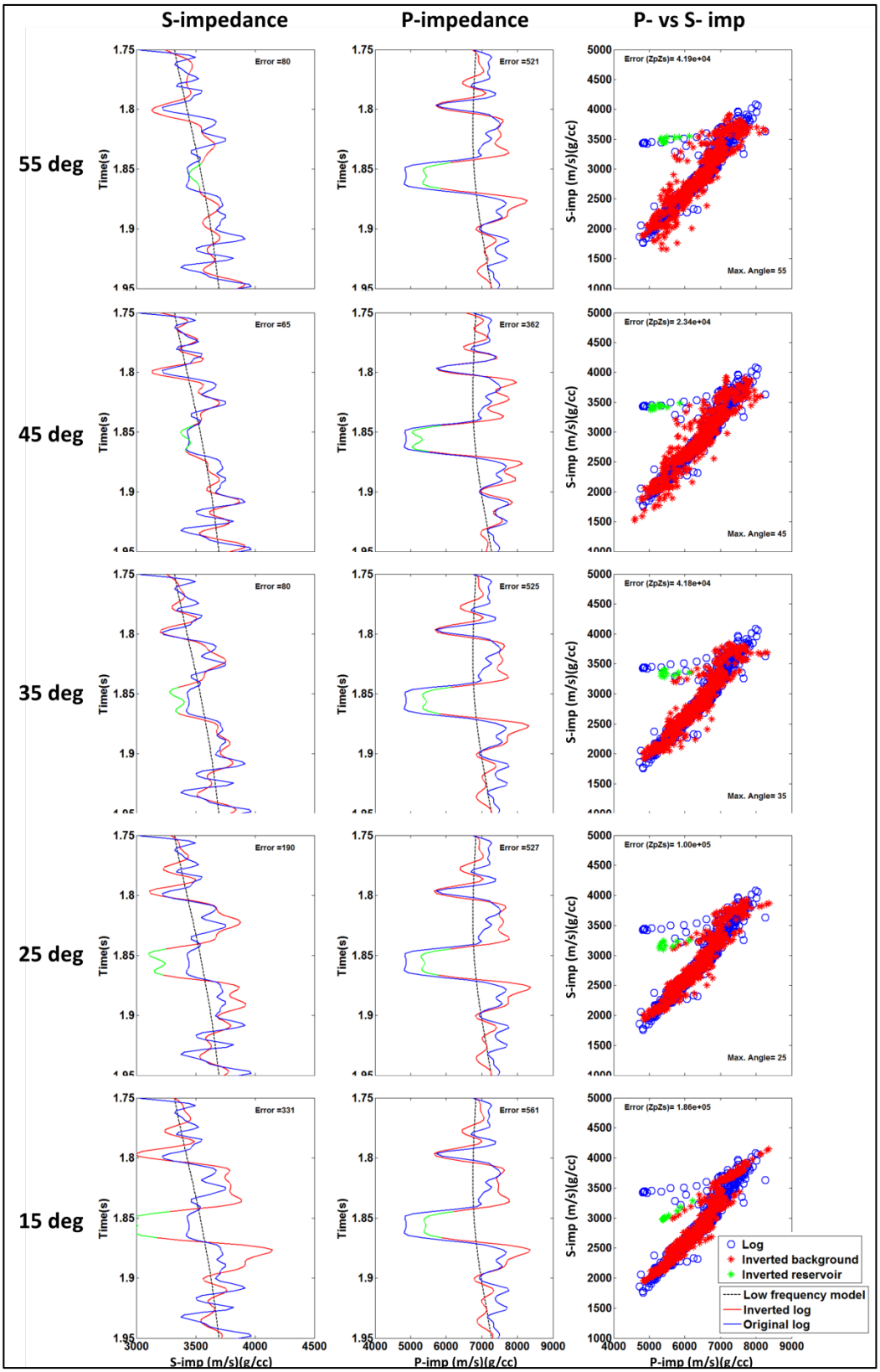

FIG. 7. Effect of reducing maximum angle of incidence in simultaneous-AVO inversion.

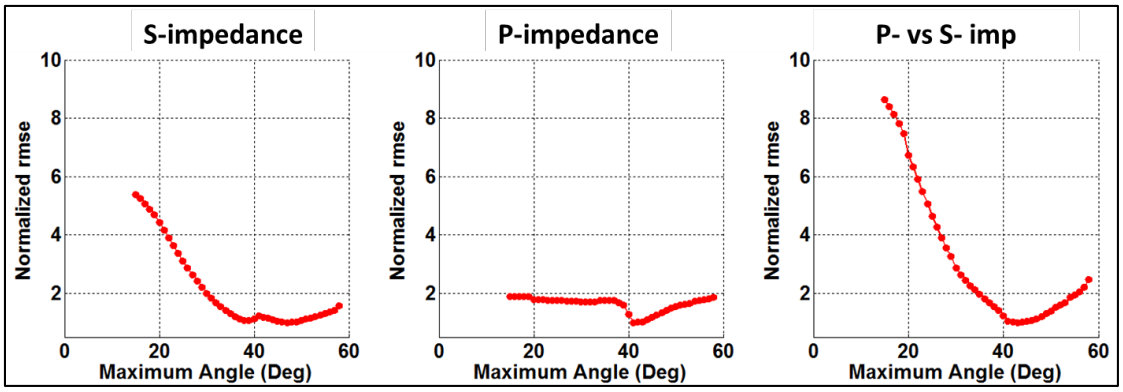

FIG. 8. Normalized RMSE for the inverted S- and P- impedances and the combined error.

Effect of random noise on simultaneous-AVO inversion

We analyzed the performance of the simultaneous inversion when varying the signal to noise ratio (from 1 to 14) while keeping the maximum angle constant at 45 degrees. Fig. 9 shows the inverted P- and S- impedance crossplot compared to the original impedances from the well and the impact of progressively increasing the signal to noise ratio. We observe that the reservoir points disperse as the S/N decreases.

The normalized RMSE, for the inverted P- and S-impedances and the combined effect of them, is shown in Fig. 10. The error bars are the standard deviation calculated after repeating the inversion several times for a particular signal to noise ratio and maximum angle. The standard deviation represents the variability of the result given the random nature of the noise.

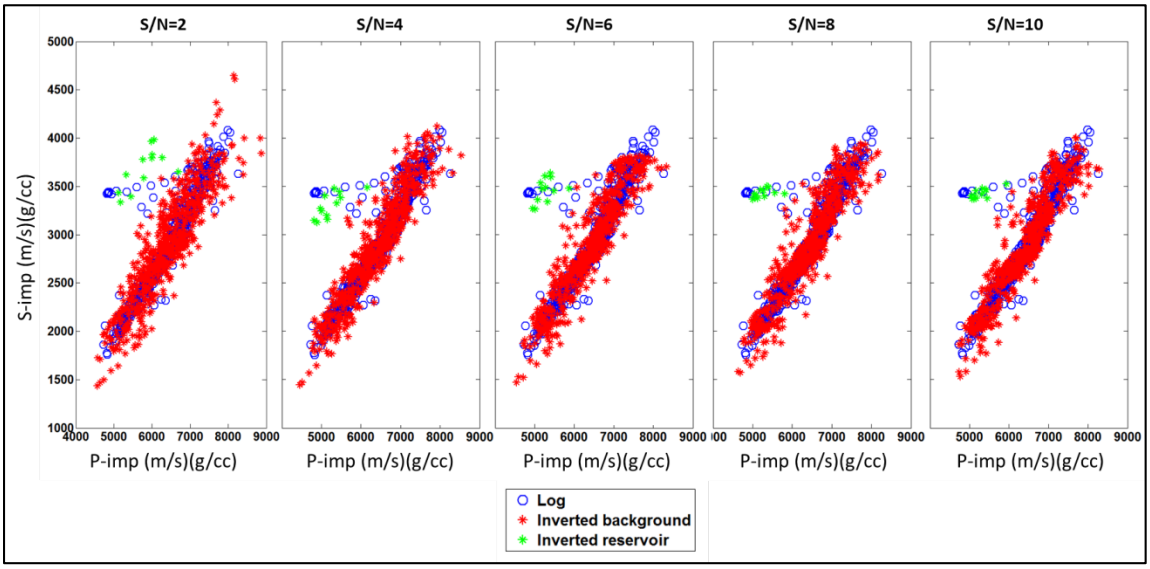

FIG. 9. Effect of random noise on inverted P- ans S- impedances obtained from simultaneous-AVO inversion. The maximum angle is 45 degrees.

The error shows that the estimation of S-impedance is more affected by random noise than the estimation of P-impedance. The combined error reflects how the P- vs S-

impedance points of the reservoir tend to be focused on the right position with S/N greater than 7.

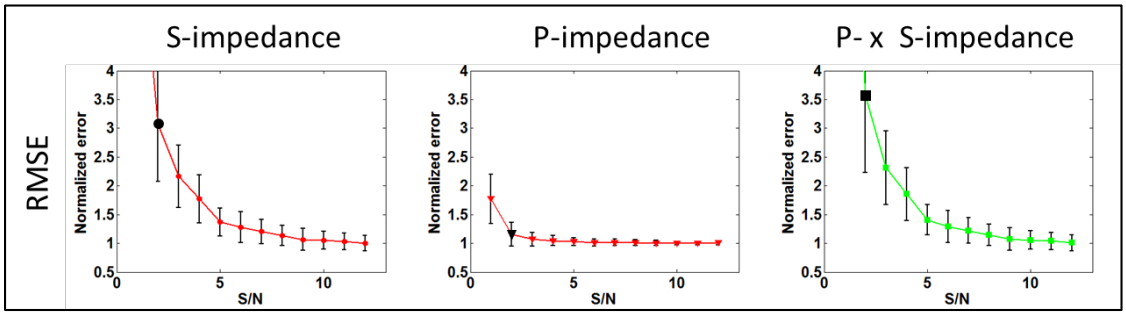

FIG. 10. Normalized RMSE when varying signal to noise ratio and keeping constant a maximum angle of 45 degrees.

Effect of random noise and maximum available offset

We plotted the RMSE as a function of S/N and maximum available angle in order to visualize the concurrent impact of these two factors on simultaneous-AVO inversion. Fig. 11 shows the normalized RMSE for both the inverted S- and P-impedance. The RMSE for S-impedance is strongly affected by S/N lower than 4. When we have maximum angles smaller than 35 degrees, the inversion result no longer improves, even if we increase the S/N to more than 4. We have the best S-impedance estimation with maximum angles around 38 degrees. The inverted S-impedance starts to decline if we use angle traces higher than 43 degrees. On the other hand, the inverted P-impedance is very stable with S/N greater than 2 for all maximum angles. The best P-impedance results arise with angles greater than 40 degrees.

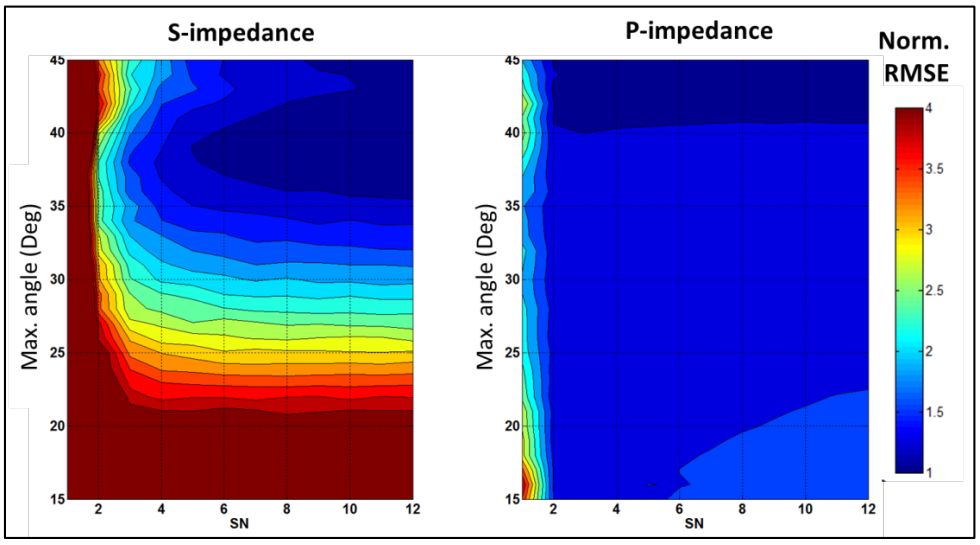

FIG. 11. Normalized RMSE as a fuction of signal to noise ratio and maximum angle of inverted S- and P- impedances.

The combined S- and P-impedance RMSE as a function of S/N and maximum angle is shown in Fig. 12. This plot gives a sense of the quality of the reservoir discrimination.

We defined four zones based on the separation of the reservoir from the background. The best results are given for angles between 40 and 45 degrees with S/N greater than 7. Acceptable separation of the reservoir from the background were obtained with maximum angles greater than 30 degrees and S/N between 3 and 7, or with S/N greater than 7 and maximum angles between 25 and 30 degrees. The separation of the reservoir is compromised (risky results zone) when we have maximum angles smaller than 30 degrees or S/N smaller than 3. Non-acceptable results are produced if the maximum angle available is smaller than 25 degrees.

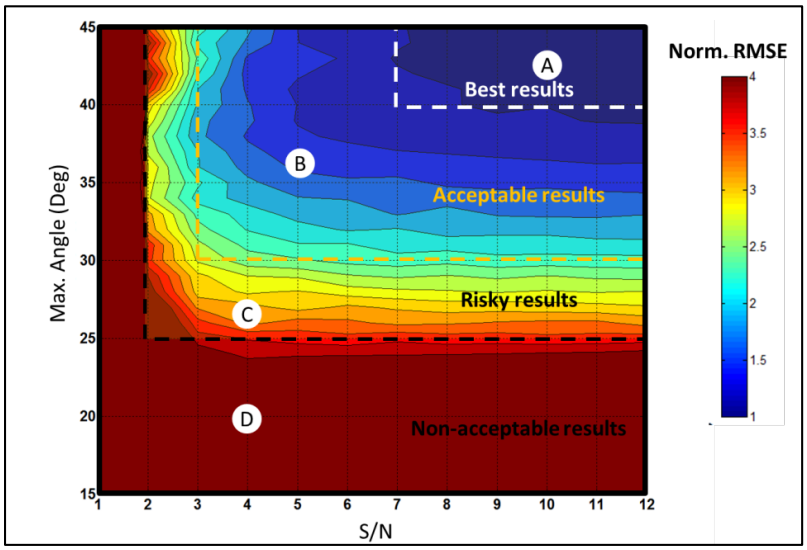

FIG. 12 Combined RMSE of inverted S- and P- impedances. Low error represents better reservoir discrimination.

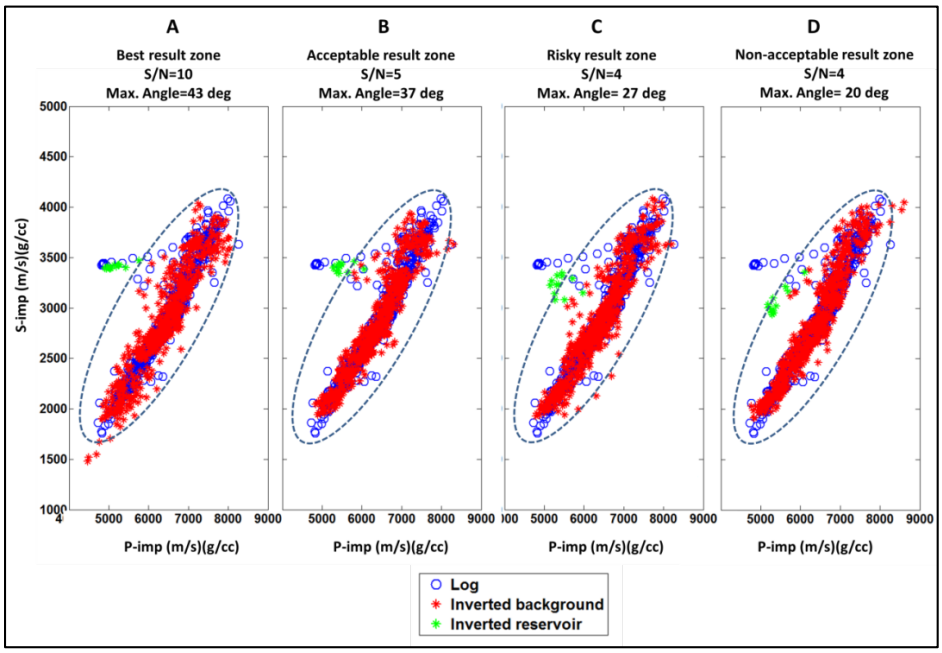

FIG. 13. Reservoir discrimination examples from the four zones defined in Fig. 12. Noise and maximum angle impact on the reservoir discrimination.

Figure 13 shows examples of the typical P- vs S-impedance crossplots we would obtain from the four zones defined in figure 12.

We can use this methodology to choose the maximum offset when we are designing a new seismic survey. For the gas target at 2280 m of depth, we may decide to acquire maximum angles of 45 degrees which corresponds to 3400 m of offset. We can also use this information to check the feasibility of applying simultaneous inversion in old data. For example, if the maximum offset was 2400 m (as large as the target depth), which corresponds to 30 degrees of angle of incidence, the results would be barely acceptable in terms of reservoir discrimination by using simultaneous inversion.

DISCUSSION

The results obtained in this experiment apply for the specific geological framework defined by the well log data. The velocities above the target, depth and impedance contrast are key variables that determine the results. Targets with other characteristics will produce different results. This work shows a methodology that can be applied to different geological settings. The impedance contrast may be a relevant factor given that the Fatti approximation fits better to the Zoeppritz equations when this property is small. Another related Fatti vs Zoeppritz issue is that the approximation error rises as the angle of incidence increases. This fact may explain why the inversion result deteriorates when we add angles of incidence greater than 45 degrees.

CONCLUSIONS

Random noise and the maximum long offset are factors that affect the performance of simultaneous-AVO inversion. The best inversion results for the gas reservoir at a 2280-m depth correspond to angles between 40 and 45 degrees with signal to noise ratios greater than 7. This scenario properly discriminates the reservoir from the background in a P- vs S-impedance crossplot. The fact that angles greater than 45 degrees deteriorate the result is probably related to the Fatti approximation error for large angles. An acceptable separation of the reservoir from the background was obtained with the following combinations of maximum angles and S/N: Max. Angles>30 and S/N=(3-7), or S/N>7 and Max. Angles=(30-40). Risky results that may compromise the discrimination of the reservoir are given by maximum angles smaller than 30 degrees and S/N smaller than 3. The results are non-acceptable if we have maximum angles smaller than 25 degrees.

The information derived from this experiment can be used for designing the maximum angle for new seismic acquisitions or for checking the feasibility to apply simultaneous inversion in old seismic data.

ACKNOWLEDGEMENTS

We thank the sponsors of CREWES for their support. We also acknowledge support from NSERC through the grant CRDPJ 461179-13. Author 1 thanks PEMEX and the government of Mexico for funding his research.

REFERENCES

Aki, K., and Richards, P., 2002, Quantitative seismology: theory and methods: Second Edition, University Science Books, Sausalito, CA.

Cambois, G.,1998, AVO attributes and noise: pitfalls of crossplotting: In SEG Expanded Abstracts, 54,2,244-247.

Cordsen, A., Galbraith, M., and Peirce, J., 2000, Planning land 3-D seismic surveys: Ed. Tulsa: Society of exploration geophysicists.

Downton, J. E. and Lines, L. R., 2001, AVO feasibility and reliability analysis: CSEG recorder, 26,6,66-73.

Fatti, J., G. Smith, P. Vail, P. Strauss, and P. Levitt, 1994, Detection of gas in sandstone reservoirs using AVO analysis: a 3D seismic case history using the Geostack technique: Geophysics, 59, 1362-1376.

Galbraith, M., 2004, A new methodology for 3D survey design: The Leading Edge, 23,10, 1017-1023.

Hampson, D. P., Russell, B. H., and Bankhead, B., 2005, Simultaneous inversion of pre-stack seismic data. In 2005 SEG Annual Meeting: Society of Exploration Geophysicists.

Stolt, R. H., and Weglein, A. B. (1985)., Migration and inversion of seismic data.Geophysics: 50,12, 2458-2472.